

## Structure and Acidic Properties of Phosphate-Modified Zirconia

D. Spielbauer, G. A. H. Mekheimer,<sup>†</sup> T. Riemer, M. I. Zaki,<sup>‡</sup> and H. Knözinger\*

*Institut für Physikalische Chemie, Universität München, Sophienstrasse 11, 80333 Munich, Germany*

*Received: November 13, 1996; In Final Form: March 24, 1997*<sup>®</sup>

Phosphate-modified zirconia was prepared by impregnation of  $\text{Zr}(\text{OH})_4$  and of  $m\text{-ZrO}_2$  with an aqueous solution of  $(\text{NH}_4)_2\text{HPO}_4$ . Similar to sulfate and tungstate, phosphate shows a strong stabilizing effect on the specific surface area and the tetragonal phase of zirconia when using  $\text{Zr}(\text{OH})_4$  as the precursor material. The adsorbed phosphate species were characterized by Raman, DRIFT, and  $^{31}\text{P}$ -MAS-NMR spectroscopies as pyrophosphates, chelate-bonded orthophosphates, and oligophosphates. Only a distortion of the geometry of the adsorbed phosphate species was found after dehydration of the materials in contrast to  $\text{ZrO}_2/\text{SO}_4$ . FT-IR spectroscopy with CO as a probe molecule was used to characterize the acidic properties of  $\text{ZrO}_2/\text{PO}_4$ . New hydroxyl groups, probably P–OH groups with enhanced protonic acidity as compared to pure zirconia but lower than that of  $\text{ZrO}_2/\text{SO}_4$ , were observed. In addition basic Zr–OH groups were observed. Furthermore, strong Lewis acidic centers (cus  $\text{Zr}^{4+}$ ), comparable to  $\text{ZrO}_2/\text{SO}_4$ , are formed by phosphate modification of zirconia.

### Introduction

The modification of zirconia by sulfate and tungstate is discussed in a number of recent publications, due to the strong acidic character of these materials and their role as possible catalysts, e.g., for the isomerization of *n*-alkanes and the alkylation of alkanes with olefins.<sup>1</sup> In the present paper the effects of the modification of zirconia by the addition of phosphate should be discussed. Whereas zirconium phosphates and their catalytic properties are well-known in the literature, phosphated zirconia was first investigated as a material for high-performance liquid chromatography (HPLC).<sup>2</sup> A most recent work describes the preparation of zirconia–phosphate aerogels<sup>3,4</sup> and their catalytic properties for the 1-butene isomerization reaction.<sup>3</sup> From their layered structure zirconium–phosphates were first discussed as ion-exchanging materials.<sup>5</sup> After calcination at 623–973 K an increasing Brønsted acidity was obtained, which was attributed to the condensation reaction between layers forming pyrophosphate ions.<sup>6</sup> These materials are able to catalyze the cis–trans isomerization of 2-butene or the dehydration of isopropyl alcohol or butanols.<sup>6,7</sup> Interesting properties were also observed after partial exchange of  $\text{H}^+$  by metal ions.<sup>7,8</sup>

The aim of the present work was to investigate the change of the structural and acidic properties of zirconia after adsorption of phosphate on (i) monoclinic zirconia and (ii) zirconium hydroxide with a subsequent calcination at 773–1073 K. Furthermore, the results will be compared with the corresponding sulfated materials.<sup>9</sup>

### Experimental Section

**Catalyst Preparation.**  $\text{Zr}(\text{OH})_4$  type XZO 632/3, dried at 393 K, was obtained from MEL, Manchester, England. Pure zirconia as a reference was prepared by calcination at  $T_1 = 773$ –973 K for 1 h. This material is denoted  $\text{Zr}(T_1)$ . Pure  $\text{Zr}(\text{OH})_4$  was suspended in an aqueous solution of  $(\text{NH}_4)_2\text{HPO}_4$  (p.a. Merck) for 1 h and subsequently dried by evaporation of the water. The dried phosphated material contained nominally 6

wt %  $\text{PO}_4$ . After calcination at  $T_2 = 773$ –1073 K, samples were obtained, which are denoted  $\text{Zr}(393)\text{P}(T_2)$ . Additional samples were prepared in the same way by phosphation of a monoclinic  $\text{ZrO}_2$ , which was obtained by calcination of the  $\text{Zr}(\text{OH})_4$  at 873 K for 4 h and which had a specific surface area of 35  $\text{m}^2/\text{g}$ . This dried material, with a nominal content of 6 wt %  $\text{PO}_4$ , was calcined at  $T_2 = 773$ –973 K and denoted  $\text{Zr}(873)\text{P}(T_2)$ .

The phosphate contents of the samples after calcination were estimated from  $^{31}\text{P}$ -MAS-NMR spectra and from the intensity of the PO bands in the Raman spectra. Whereas for the samples  $\text{Zr}(393)\text{P}(T_2)$  no loss of phosphate was found for any calcination temperature  $T_2$ , the phosphate content decreases from 6 wt %  $\text{PO}_4$  to about 3.5–4 wt % for the samples  $\text{Zr}(873)\text{P}(T_2)$  by increasing the calcination temperature  $T_2$  from 773 to 873 K.

**Surface Area Measurements and X-ray Diffraction.** The specific surface areas were measured by the BET method with a Sorptomatic 1800 from Carlo Erba. X-ray diffraction was performed by a Siemens D5000 Diffraktometer with Ni-filtered Cu K $\alpha$  radiation under ambient conditions. The crystallographic phase compositions were calculated by the method of Toraya et al.<sup>10</sup>

**Laser Raman Spectroscopy.** For laser Raman spectroscopy (LRS) an in situ Raman cell that was described previously<sup>11</sup> was used. This cell allowed the heating of the samples at temperatures up to 770 K in the presence of either static or flowing gas atmospheres of any kind. Samples were pressed into special stainless steel holders. Raman spectra were recorded on a Dilor (OMARS 89) spectrometer which was equipped with a Princeton Applied Instruments optical multichannel analyzer (OMA). The Raman spectra were excited by the 488 nm line of an Ar<sup>+</sup>-ion laser model series 2020 from Spectra Physics. The laser power at the sample position was 30 mW. Spectra were recorded using the scanning multichannel technique (SMT).<sup>12</sup>

**Infrared Spectroscopy.** Transmission IR and DRIFT spectra were recorded with a Bruker IFS-88 FT-IR spectrometer equipped with a liquid nitrogen cooled MCT detector. For spectra in transmission, a specially designed cell, which was described in detail elsewhere,<sup>13</sup> allows in situ pretreatment at temperatures up to 773 K and permits recording of spectra between 80 and 300 K in vacuo ( $\leq 10^{-5}$  mbar) or in static gas atmosphere. The samples were prepared as thin self-supporting

\* Author to whom correspondence should be addressed.

<sup>†</sup> On leave from Department of Chemistry, Faculty of Science, Minia University, El-Minia, Egypt.

<sup>‡</sup> Department of Chemistry, Kuwait University, Kuwait.

<sup>®</sup> Abstract published in *Advance ACS Abstracts*, May 15, 1997.

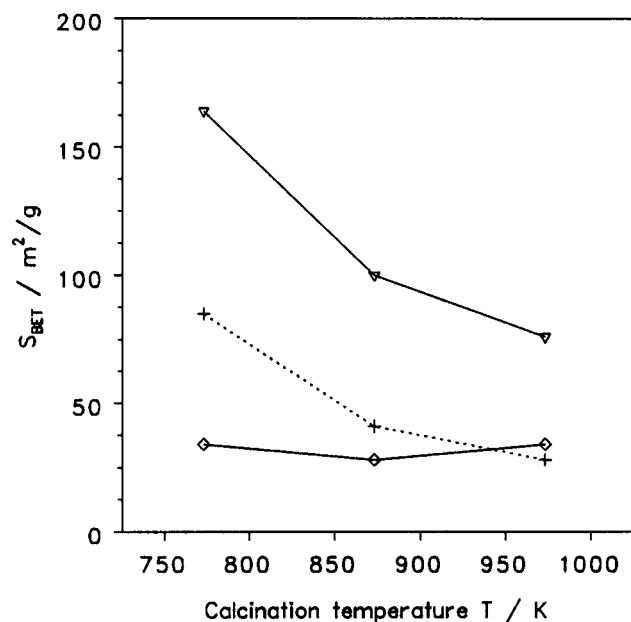


**Figure 1.** BET surface areas of Zr(T<sub>1</sub>) (+), Zr(393)P(T<sub>2</sub>) (∇), and Zr(873)P(T<sub>2</sub>) (◇).

wafers (typically ca. 20 mg/cm<sup>2</sup>). These specimens were pretreated in situ by calcination at 723 K in O<sub>2</sub> for 1 h and subsequent evacuation at 723 K for 1 h. The spectra were recorded with a spectral resolution of 2 cm<sup>-1</sup>. CO (≥99.997%, Linde AG) was used as a probe molecule. CO was further purified by passing it through an Oxisorb cartridge. Adsorption of CO was carried out at 77 K by a stepwise increase of the CO pressure from 0.5 to 40–55 mbar.

For DRIFT spectra a Spectratech cell was used, which allows pretreatment in static or flowing gas atmospheres up to 693 K.

**Solid State NMR.** NMR measurements were performed on a Bruker MSL 400 NMR spectrometer with a magnetic field strength of 9.4 T and a <sup>31</sup>P-NMR frequency of 161.96 MHz. A sample of 85% H<sub>3</sub>PO<sub>4</sub> was used as an external standard with an accuracy of ±0.2 ppm. The MAS rotation frequency was 8 kHz, and proton decoupling was applied. The samples were pretreated in a quartz reactor at 723 K in O<sub>2</sub> for 1 h and then evacuated (<10<sup>-3</sup> mbar) at 723 K for 1 h. The powder samples were subsequently transferred into NMR tubes connected to the reactor tube. These NMR tubes were sealed off without exposure to the atmosphere.

## Results and Discussion

**BET Surfaces and X-ray Diffraction.** Phosphate modification of Zr(OH)<sub>4</sub> for preparation of the samples Zr(393)P(T<sub>2</sub>) increases the surface area as compared to the pure zirconia samples Zr(T<sub>1</sub>) (see Figure 1). Increasing the calcination temperature lowers the surface areas for pure and phosphate-modified Zr(OH)<sub>4</sub>. No loss of surface area with calcination temperature was observed for the samples Zr(873)P(T<sub>2</sub>), suggesting that the adsorption of phosphate on ZrO<sub>2</sub> suppresses sintering and growth of the crystallites. A similar effect was found for sulfated ZrO<sub>2</sub>.<sup>14</sup>

X-ray diffraction of the samples Zr(393)P(T<sub>2</sub>) showed predominantly (>90%) the pattern of tetragonal ZrO<sub>2</sub>, even at the highest calcination temperature. At temperatures T<sub>2</sub> up to 873 K additional broad reflections of amorphous zirconia were observed, indicating a strong perturbation of the crystallization of ZrO<sub>2</sub> by the presence of phosphate. Because of the thermal stability of phosphate the phase transition to *m*-ZrO<sub>2</sub> was largely suppressed even at this high temperature in contrast to sulfated

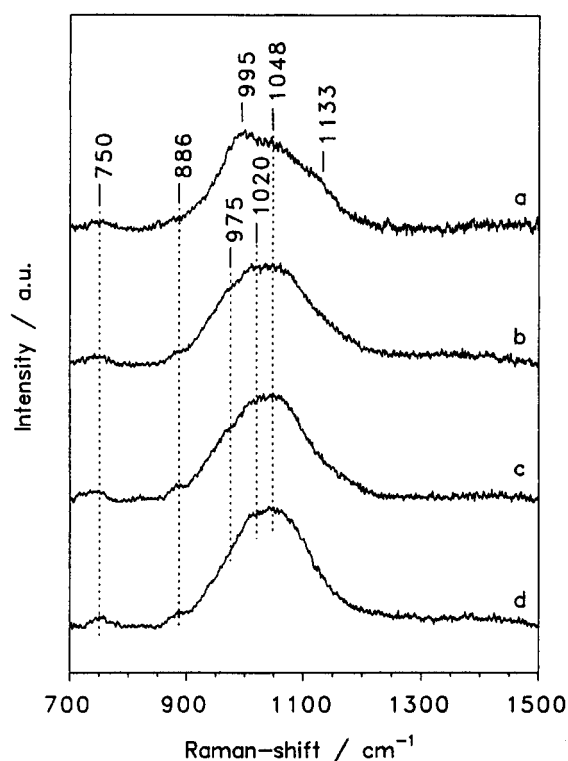


**Figure 2.** Raman spectra of Zr(393)P(T<sub>2</sub>) at ambient conditions with (a) T<sub>2</sub> = 773 K, (b) 873 K, (c) 973 K, and (d) 1073 K.

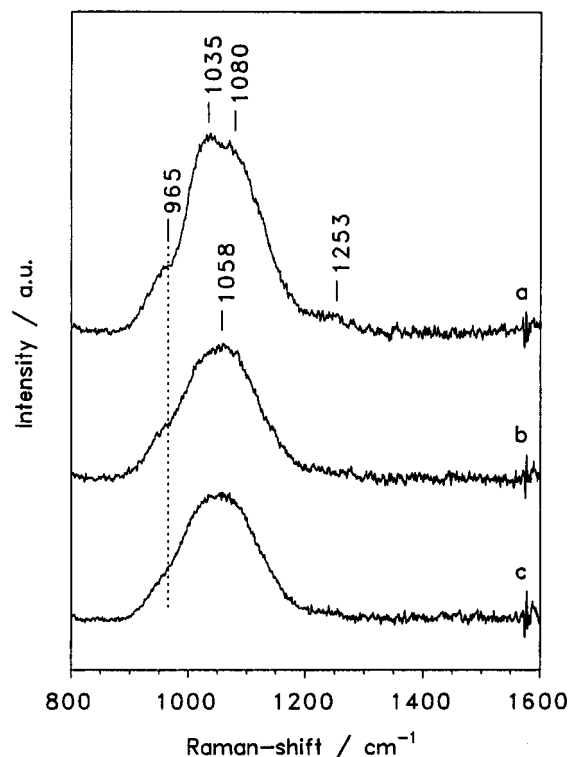
Zr(OH)<sub>4</sub>.<sup>14</sup> The samples Zr(T<sub>1</sub>) and Zr(873)P(T<sub>2</sub>) show predominantly (>90%) the pattern of *m*-ZrO<sub>2</sub>.

**Structure of Adsorbed Phosphate Species. Raman Spectra of Hydrated Samples.** Since the tetragonal and the monoclinic phases of zirconia show intense bands of Zr–O vibrations up to 650 cm<sup>-1</sup> in the Raman spectra,<sup>15</sup> the discussion must be limited to P–O stretching vibrations greater than 750 cm<sup>-1</sup>. Consistent with the results from X-ray diffraction, the Raman spectra of samples Zr(T<sub>1</sub>) and Zr(873)P(T<sub>2</sub>) predominantly show the bands of the monoclinic phase, whereas for samples Zr(393)P(T<sub>2</sub>) mostly bands of the tetragonal phase were observed, besides a high background from amorphous parts present at low calcination temperatures T<sub>2</sub>.

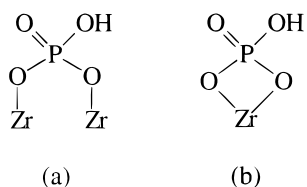
Because of this background and the intense Zr–O bands, the spectral ranges of P–O vibrations shown in the figures are corrected by background subtraction. Figure 2 shows the Raman spectra of the samples Zr(393)P(T<sub>2</sub>) at ambient conditions. Calcination at 773 K (spectrum a in Figure 2) causes a band at 995 cm<sup>-1</sup> with shoulders at 1048 and 1133 cm<sup>-1</sup> and an additional weak band at 750 cm<sup>-1</sup>. Corresponding to literature data of Na<sub>4</sub>P<sub>2</sub>O<sub>7</sub> (see Table 1), these bands can be attributed to pyrophosphates (P<sub>2</sub>O<sub>7</sub><sup>4-</sup>). Different frequencies were reported for Raman spectra of cubic ZrP<sub>2</sub>O<sub>7</sub><sup>19</sup> with bands at 990, 1000, 1094, and 1200 cm<sup>-1</sup>. A weak band at 886 cm<sup>-1</sup>, which increases with calcination temperature T<sub>2</sub> (see spectra b–d in Figure 2), suggests the presence of an additional chelated or doubly bridged PO<sub>4</sub> species (vide infra) (Chart 1), bearing an isolated P–OH group. Raising the calcination temperature decreases the intensity of the band at 995 cm<sup>-1</sup> whereas the band at 1048 cm<sup>-1</sup> is simultaneously increased together with a new shoulder at 1020 cm<sup>-1</sup>. As the intensity of the band at 750 cm<sup>-1</sup> shows no change with T<sub>2</sub>, further condensation of the pyrophosphates into oligophosphates can obviously be excluded. Corresponding to this and the results of the <sup>31</sup>P-MAS-NMR spectra (vide infra), the observed changes in the Raman spectra rather suggest a modification of the chemical environ-

TABLE 1: P–O Stretching Vibrations of Some Phosphorous–Oxy Compounds

reference compound	symmetry		ref
Na <sub>2</sub> PO <sub>4</sub>	<i>T<sub>d</sub></i>	938, 1017	16
K <sub>2</sub> HPO <sub>4</sub>		1084, 970 (PO <sub>3</sub> ), 891 (P–OH)	16
OPF <sub>3</sub>	<i>C<sub>3v</sub></i>	1415	16
(Zr–O) <sub>3</sub> P–OH		1140, 1105,	6
(α-Zr(HPO <sub>4</sub> ) <sub>2</sub> ·H <sub>2</sub> O)		910 (P–OH)	
KH <sub>2</sub> PO <sub>4</sub>	<i>C<sub>2v</sub></i>	1155, 1071 (PO <sub>2</sub> ), 1027, 877 (P(OH) <sub>2</sub> )	16
[Co(NH <sub>3</sub> ) <sub>4</sub> PO <sub>4</sub> ]·2H <sub>2</sub> O	<i>C<sub>2v</sub></i> (chelate)	1109, 1043, 918, 895	17
[Co(NH <sub>3</sub> ) <sub>4</sub> (OH <sub>2</sub> )(OPO <sub>3</sub> H)]J·2H <sub>2</sub> O	<i>C<sub>s</sub></i>	1090, 1044, 982, 878 (P–OH)	17
Na <sub>4</sub> P <sub>2</sub> O <sub>7</sub>	<i>C<sub>2v</sub></i>	1120–1150 (PO <sub>3</sub> ), 1020 (PO <sub>3</sub> ), 915 (ν <sub>as</sub> , P–O–P), 730 (ν <sub>s</sub> , P–O–P)	18

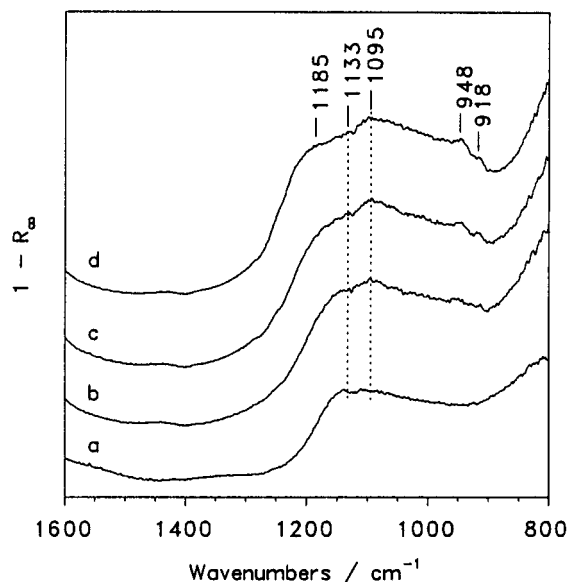
Figure 3. Raman spectra of Zr(873)P(*T*<sub>2</sub>) at ambient conditions with (a) *T*<sub>2</sub> = 773 K, (b) 873 K, and (c) 973 K.

#### CHART 1: Model of Adsorbed (a) Doubly Bridged and (b) Chelating PO<sub>4</sub> Groups



ment of the adsorbed pyrophosphate species, namely a more covalent bonding character.

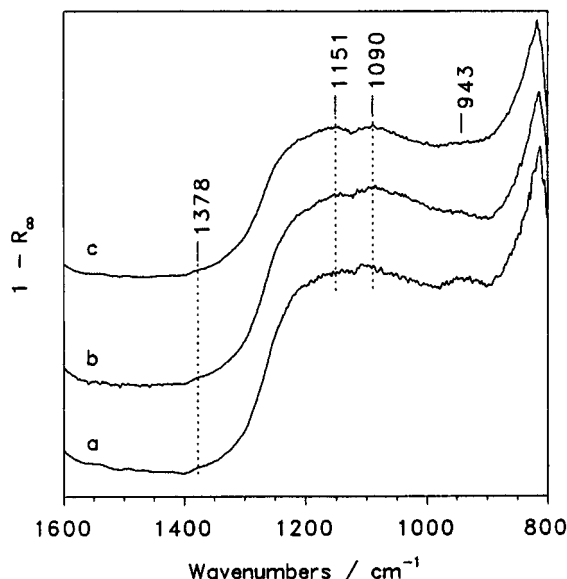
The P–O bands in the Raman spectra of the samples Zr(873)P(*T*<sub>2</sub>) appear at higher wavenumbers (see Figure 3). The sample calcined at 773 K (see spectrum a in Figure 3) shows a band at 1035 cm<sup>−1</sup> with additional shoulders at 965, 1080, and 1253 cm<sup>−1</sup>. Due to the results of the <sup>31</sup>P-MAS-NMR spectra (vide infra) the P–O bands in the Raman spectra of these samples could also be attributed to pyrophosphates. The characteristic stretching vibration of the P–O–P groups at about 750 cm<sup>−1</sup> could not be identified for these samples, because of the superposition of an overtone at about 760 cm<sup>−1</sup> of Zr–O fundamental vibrations of monoclinic ZrO<sub>2</sub>. Increasing the calcination temperature to 873 K decreases the total intensity of the P–O bands. The band at 1035 cm<sup>−1</sup> and the shoulders at 965 and 1253 cm<sup>−1</sup> are less pronounced at higher temperatures *T*<sub>2</sub>.

Figure 4. DRIFT spectra of Zr(393)P(*T*<sub>2</sub>) at ambient conditions with (a) *T*<sub>2</sub> = 773 K, (b) 873 K, (c) 973 K, and (d) 1073 K.

It should be noted that further statements about the coordination geometry of the pyrophosphate and oligophosphate species are not possible due to the line width of the P–O bands in the obtained spectra of the samples.

**DRIFT Spectra of Hydrated Samples.** The DRIFT spectrum of Zr(393)P(773) (see spectrum a in Figure 4) shows bands at 1133 and 1095 cm<sup>−1</sup>. These frequencies are in agreement with IR data of amorphous ZrP<sub>2</sub>O<sub>7</sub>,<sup>6,20</sup> whereas an intense band at 760–780 cm<sup>−1</sup>, which could also be identified in the spectra of pure ZrO<sub>2</sub> samples, prevents the identification of P–O–P bands at about 750 cm<sup>−1</sup>. Raising the calcination temperature *T*<sub>2</sub> increases the intensity of the band at 1095 cm<sup>−1</sup>, and new bands at 1185, 948, and 918 cm<sup>−1</sup> are observed (see spectra b–d in Figure 4). The bands at 1185, 1095, and 948 cm<sup>−1</sup> are tentatively attributed to another kind of pyrophosphate species with a different chemical environment. The band at 918 cm<sup>−1</sup> is probably related to the band at 886 cm<sup>−1</sup> observed in the Raman spectra (see spectra b–d in Figure 2). These bands are assigned respectively to the antisymmetric and symmetric O–P–O stretching vibration of a doubly bridging (Chart 1a) or chelating PO<sub>4</sub> group (Chart 1b), as, e.g., in the complex [Co(NH<sub>3</sub>)<sub>4</sub>PO<sub>4</sub>]·2H<sub>2</sub>O with chelate type phosphate with bands at 918 and 895 cm<sup>−1</sup> (see Table 1). Chelate-bonded PO<sub>4</sub> groups with PO<sub>2</sub><sup>−</sup> groups were proposed by Boyse and Ko<sup>3</sup> on the surface of calcined ZrO<sub>2</sub>/PO<sub>4</sub> gels.

The DRIFT spectra of the samples Zr(873)P(*T*<sub>2</sub>) show bands at 1151, 1090, and 943 cm<sup>−1</sup> (see Figure 5), which can be attributed to pyrophosphate species.<sup>6,20</sup> The intensity of the bands decreases—consistent with the Raman spectra—by raising the calcination temperature *T*<sub>2</sub> from 773 to 873 K (see spectra



**Figure 5.** DRIFT spectra of  $\text{Zr}(873)\text{P}(T_2)$  at ambient conditions with (a)  $T_2 = 773$  K, (b) 873 K, and (c) 973 K.

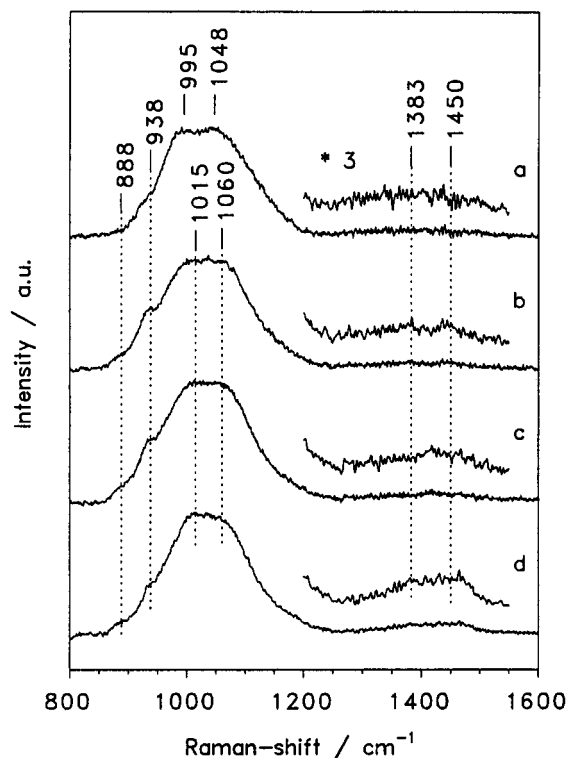


**Figure 6.** Raman spectra of  $\text{Zr}(393)\text{P}(T_2)$  after calcination at 773 K (1 h), measured at 773 K with (a)  $T_2 = 773$  K, (b) 873 K, (c) 973 K, and (d) 1073 K.

a and b in Figures 3 and 5). No bands are observed for chelate type  $\text{PO}_4$  species, which is again consistent with the Raman spectra.

**Raman Spectra of Dehydrated Samples.** The Raman spectra (recorded at 773 K) of dehydrated samples  $\text{Zr}(393)\text{P}(T_2)$  showed a shift of the low-frequency bands at 975 and 1020  $\text{cm}^{-1}$  to 938 and 1015  $\text{cm}^{-1}$ , respectively, whereas the band at 1048  $\text{cm}^{-1}$  is shifted to 1060  $\text{cm}^{-1}$  (see Figure 6). The observed frequency shifts are increased by about 10  $\text{cm}^{-1}$  when cooling the samples to room temperature (not shown), and the bands at 750 and 886  $\text{cm}^{-1}$ , which could not be identified in the spectra measured at 773 K, were then detected. From these results, a modification of the coordination symmetry of the phosphate

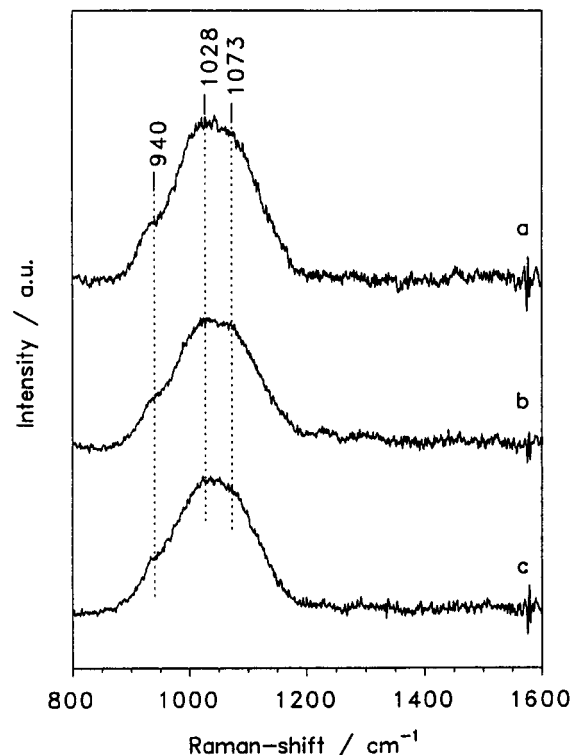


**Figure 7.** Raman spectra of  $\text{Zr}(873)\text{P}(T_2)$  after calcination at 773 K (1 h), measured at 773 K with (a)  $T_2 = 773$  K, (b) 873 K, and (c) 973 K.

**TABLE 2: Chemical Shifts  $\delta_P$  of Some Crystalline Na-Phosphates and Zirconium Phosphor-Oxy Compounds**

reference compound	$\delta_P/\text{ppm}$	ref
$\text{Na}_3\text{PO}_4 \cdot 12\text{H}_2\text{O}$	6.9	22
$\text{Na}_2\text{HPO}_4$	-0.2	22
$\text{NaH}_2\text{PO}_4 \cdot 2\text{H}_2\text{O}$	0.4	22
$\text{Na}_4\text{P}_2\text{O}_7$	1.3, 2.9	22
$\text{Na}_3\text{HP}_2\text{O}_7 \cdot \text{H}_2\text{O}$	-2.3, -5.0	22
$\text{Na}_2\text{H}_2\text{P}_2\text{O}_7$	-8.2	22
$\text{Na}_5\text{P}_3\text{O}_{10}$	1.2, -7.4	22
$\text{Na}_4\text{P}_4\text{O}_{12} \cdot 4\text{H}_2\text{O}$	-19.7, -22.4	22
$\alpha\text{-Zr}(\text{HPO}_4)_2 \cdot \text{H}_2\text{O}$	-16.6	26
$\epsilon\text{-Zr}(\text{HPO}_4)_2$	-21.7	26
$\text{ZrP}_2\text{O}_7^a$	-34 to -43	26

<sup>a</sup> Prepared by evacuation of  $\alpha\text{-Zr}(\text{HPO}_4)_2 \cdot \text{H}_2\text{O}$  or  $\epsilon\text{-Zr}(\text{HPO}_4)_2$  at 1323 or 1473 K, respectively.

species on the zirconia surface, as observed for sulfated zirconia by drastic changes in the Raman and IR spectra,<sup>14,21</sup> can probably be excluded. However, the small shifts of the frequencies of the P-O stretching vibrations after dehydration of the samples suggest gradual changes of the molecular geometries and of the P-O bond orders. Samples calcined at higher temperature (see spectra b-d in Figure 6) show weak bands at 1380 and 1450  $\text{cm}^{-1}$ , possibly indicating the presence of carbonates.

In the Raman spectra of the samples  $\text{Zr}(873)\text{P}(T_2)$ , measured at 773 K (see Figure 7), similar bands at 940 (sh), 1028, and 1073 (sh) are obtained, whereas no bands between 1200 and 1600  $\text{cm}^{-1}$  were observed.

**<sup>31</sup>P-MAS-NMR Spectra of Dehydrated Samples.** As can be seen in Table 2, which summarizes the chemical shifts  $\delta_P$  of some crystalline Na-phosphates,<sup>22</sup>  $\delta_P$  shifts to negative values with increasing chain length ( $\text{PO}_4^{3-} < \text{P}_2\text{O}_7^{4-} < \text{P}_3\text{O}_{10}^{5-}$ ...) and with increasing degree of protonation ( $\text{P}_2\text{O}_7^{4-} < \text{HP}_2\text{O}_7^{3-} < \text{H}_2\text{P}_2\text{O}_7^{2-}$ ). No simple trends can be observed for the presence of crystal water, since the crystalline structure also

**TABLE 3: Chemical Shifts  $\delta_P$  of Dehydrated  $ZrO_2/PO_4$  Samples**

sample	$T_2/K$	$\delta_P/ppm$			
Zr(393)P( $T_2$ )	773	-6.9	-12 (sh, m)	-17 (sh, w)	
	873	-6.9 (sh, m)	-11.2	-17 (sh, m)	
	973	-6.9 (sh, w)	-11.5	-17 (sh, m)	
	1073		-12.8		
Zr(873)P( $T_2$ )	773	-18	-31		
	873	-17	-31		
	973	-16	-31		

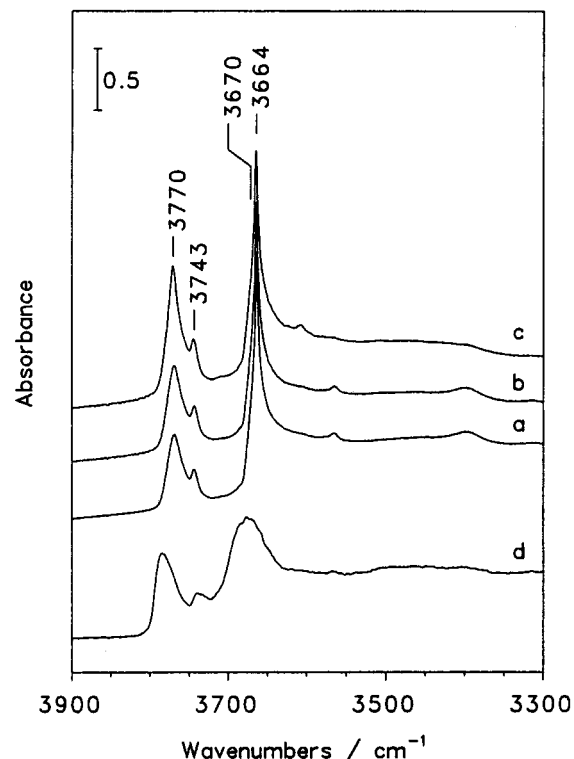
changes. More negative chemical shifts were found for cyclic phosphates<sup>23</sup> and branched phosphates<sup>23</sup> as well as phosphate in  $SiO_2$ ,<sup>23</sup>  $AlPO_4$ ,<sup>24</sup> and phosphate-modified USY zeolites<sup>25</sup> with a more covalent character of the P—O—Si or P—O—Al bonds. However, for zirconium phosphates and zirconium pyrophosphate ( $ZrP_2O_7$ ) with enhanced covalent character of the P—O—Zr bonds, strong negative chemical shifts were observed<sup>26,27</sup> (see Table 2).

The results of the  $^{31}P$ -MAS-NMR spectra of the dehydrated phosphated zirconia samples are presented in Table 3. Zr(393)P(773) shows a broad signal at -6.9 ppm with a shoulder at about -12 ppm. Corresponding to the literature data of crystalline phosphates (see Table 2) and the results of the Raman and DRIFT spectra, the signal at -6.9 ppm is attributed to predominant ionic, protonated pyrophosphate species. The shoulder at -12 ppm suggests the presence of more highly condensed phosphates and/or pyrophosphates with a more covalent P—O—Zr bond. Raising the calcination temperature  $T_2$  to 873 K increases the intensity of the signal at about -12 ppm, whereas the signal at ca. -7 ppm decreases and an additional shoulder at -17 ppm could be observed. As the intensity of the P—O—P stretching vibration at  $750\text{ cm}^{-1}$  is largely equal in the Raman spectra of all samples Zr(393)P( $T_2$ ), the observed shift of the signals in  $^{31}P$ -MAS-NMR spectra are probably not caused by the condensation to oligophosphates, but rather by the transformation of ionic pyrophosphates to more covalently bonded species, as observed for zirconium phosphates.<sup>2,26</sup> Calcination at 973 and 1073 K decreases the signal intensity at -7 ppm and increases that of the signal at -17 ppm further. For the sample Zr(393)P(1073) no signal of ionic pyrophosphate at -7 ppm was observed.

In the spectra of the samples Zr(873)P( $T_2$ ) two broad signals at -18 to -16 ppm and at -31 ppm were obtained (see Table 3). The total intensity of the signals decreases by raising the calcination temperature from 773 to 873 K. The low specific surface area of the phosphate-free precursor material results in an enhanced concentration of phosphate species at the surface, which favors the condensation to oligophosphates. This condensation and the covalent character of the P—O—Zr bond causes the shift of the signals in  $^{31}P$ -MAS-NMR spectra to more negative values.

**Acidity of  $ZrO_2/PO_4$  FT-IR Spectra with Adsorbed Carbon Monoxide.** *Hydroxyl Stretching Region ( $3300\text{--}3900\text{ cm}^{-1}$ ).* After dehydration of pure zirconia Zr(873) two bands at  $3780$  and  $3680\text{ cm}^{-1}$  are observed in the IR spectrum (see spectrum d in Figure 8), which are assigned to isolated and bridging surface OH groups, respectively, of monoclinic zirconia.<sup>28,29</sup> An additional weak band at  $3740\text{ cm}^{-1}$ , also found in the spectra of the phosphated samples, is probably caused by small amounts of silica,<sup>30</sup> which is an impurity of the used  $Zr(OH)_4$ . Addition of CO causes a shift of the band of acidic OH groups at  $3680$  to  $3610\text{ cm}^{-1}$ , whereas the other two bands of basic OH groups are not affected (see Table 4).

The IR spectra of phosphated  $m$ - $ZrO_2$  (Zr(873)P( $T_2$ )) (see spectra a–c in Figure 8) show bands at  $3770$ ,  $3743$ , and  $3664$

**Figure 8.** FT-IR spectra of Zr(873)P( $T_2$ ) with (a)  $T_2 = 773\text{ K}$ , (b)  $873\text{ K}$ , (c)  $973\text{ K}$  and (d) Zr(873) after calcination at  $723\text{ K}$  (1 h), measured at  $77\text{ K}$ .**TABLE 4: Hydroxyl Stretching Frequencies of Acidic OH Groups of  $ZrO_2$ ,  $ZrO_2/PO_4$ , and  $ZrO_2/SO_4$  prior to and after Addition of CO Under Saturation Conditions at  $77\text{ K}$** 

sample	$T_2/K$	$\nu_{OH}/\text{cm}^{-1}$	$\nu_{OH-CO}/\text{cm}^{-1}$	$\Delta\nu_{OH}/\text{cm}^{-1}$
Zr(873)		3680	3610	-70
Zr(873)P( $T_2$ )	773	3664	3489	-175
	873	3664	3498	-166
	973	3664	3533 (sh), 3502	-131, -162
Zr(393)P( $T_2$ )	773	3664	~3530	-134
	873	3664	~3500	-164
	973	3660	~3500	-160
$ZrO_2/SO_4^a$	873	3640	3480, 3420	-160, -220
	873	3640	3480, 3420	-160, -220

<sup>a</sup> Prepared by calcination of sulfated  $Zr(OH)_4$  at  $873\text{ K}$  (1 h).

<sup>b</sup> Prepared by calcination of sulfated Zr(873) at  $873\text{ K}$  (1 h).

$\text{cm}^{-1}$  prior to the adsorption of CO. A weak shoulder at ca.  $3670\text{ cm}^{-1}$  can be clearly identified as an additional OH band after the adsorption of CO (vide infra). Raising the calcination temperature  $T_2$  causes an increased intensity of the band at  $3770\text{ cm}^{-1}$  as compared to the band at  $3664\text{ cm}^{-1}$ . The stretching frequencies of the OH bands of the phosphated samples may suggest an assignment to Zr—OH groups with enhanced acidity as compared to pure  $m$ - $ZrO_2$  as indicated by the shift of the bands by about  $-10\text{ cm}^{-1}$ . However, (i)  $\alpha$ -zirconium phosphate shows a band at  $3660\text{--}3670\text{ cm}^{-1}$ ,<sup>31</sup> which was attributed to POH groups; (ii) the small line width of the bands at  $3770$  and  $3664\text{ cm}^{-1}$  as compared to pure zirconia (Zr(873)) or sulfated zirconia<sup>9</sup> under the same conditions suggests the presence of isolated hydroxyl groups with OH bands, which are not broadened by the inhomogeneity of the surface; (iii) two bands at  $1200$  and  $1270\text{ cm}^{-1}$  (not shown), characteristic of P—O—H (out-of-plane) deformation vibrations,<sup>31,32</sup> suggest the formation of POH groups.

Figure 9 shows the transmission IR spectra of the sample Zr(873)P(873) after the exposure to increasing pressures of CO, which induces the formation of a new, broad band at  $3498\text{ cm}^{-1}$ ,

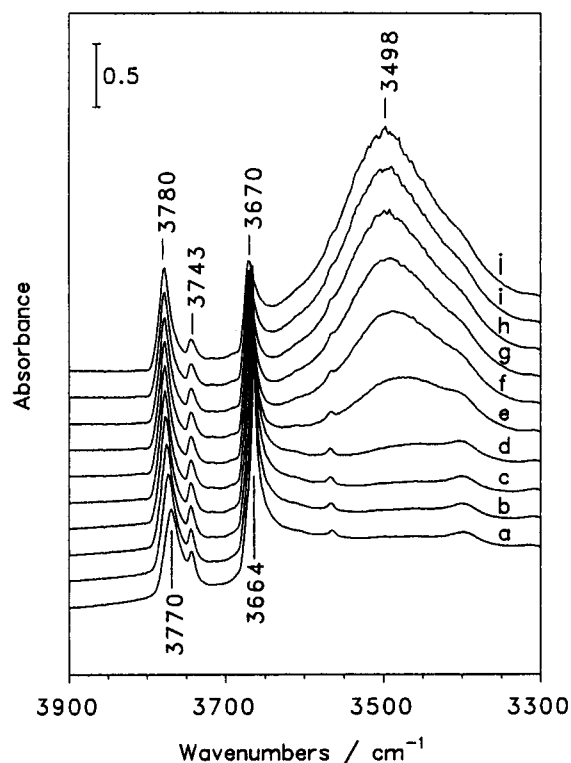


**Figure 9.** FT-IR spectra of the hydroxyl stretching region of Zr(873)P(873) after calcination at 723 K (1 h) after adsorption of (a) 0.0, (b) 0.5, (c) 1.0, (d) 3.0, (e) 5.0, (f) 10, (g) 20, (h) 30, (i) 40, and (j) 55 mbar CO, measured at 77 K.

whereas the band at  $3664\text{ cm}^{-1}$  simultaneously decreases in intensity. The enhanced shift of the OH band by  $166\text{ cm}^{-1}$ , as compared to pure *m*-ZrO<sub>2</sub> (see Table 4), indicates an increased protonic acidity of zirconia by phosphate modification. It is noteworthy that the band at  $3664\text{ cm}^{-1}$  does not completely disappear under saturation conditions of adsorbed CO (55 hPa), but a residual band at  $3670\text{ cm}^{-1}$ , probably Zr–OH groups, can be identified. Furthermore, the band at  $3770\text{ cm}^{-1}$  is not shifted to lower wavenumbers by the addition of CO and is consequently attributed to Zr–OH groups, whereas the band at  $3664\text{ cm}^{-1}$  is assigned to P–OH groups (vide supra). A similar band of P–OH groups at  $3670\text{ cm}^{-1}$  was observed in the IR spectrum of phosphate-modified Aerosil silica surface.<sup>33</sup> Adsorption of benzene shows enhanced protonic acidity for these groups, as compared to the pure support.

The IR spectra of the samples Zr(393)P(*T*<sub>2</sub>) (see Figure 10) show bands of unperturbed OH groups at  $3770$ ,  $3743$ ,  $3670$  (sh), and  $3664\text{ cm}^{-1}$  with enhanced line widths as compared to the samples Zr(873)P(*T*<sub>2</sub>) (see spectra a–c in Figure 8). The intensity of the band at  $3770\text{ cm}^{-1}$  increases as compared to the band at  $3664\text{ cm}^{-1}$ , similar to the samples Zr(873)P(*T*<sub>2</sub>), with increasing calcination temperature *T*<sub>2</sub>. Since the samples Zr(393)P(*T*<sub>2</sub>) predominantly consist of *t*-ZrO<sub>2</sub>, which shows only a single OH band at  $3682\text{ cm}^{-1}$ ,<sup>29</sup> the previously suggested assignment of the band at  $3770\text{ cm}^{-1}$  to Zr–OH groups may be uncertain. However, after evacuation of  $\alpha$ -zirconium phosphate at  $820\text{ K}$ <sup>31</sup> additional bands at  $3700$  and  $3770\text{ cm}^{-1}$  were assigned to Zr–OH bands, besides the band of POH groups at  $3660$ – $3670\text{ cm}^{-1}$ . These results on  $\alpha$ -zirconium phosphate are possibly indicative for the formation of a kind of bulk zirconium phosphate on the phosphate-modified zirconia. In contrast to samples Zr(873)P(*T*<sub>2</sub>), only one band of P–O–H (out-of-plane) deformation vibrations was found in the spectra of Zr(393)P(*T*<sub>2</sub>) at  $1240$  (*T*<sub>2</sub> =  $773\text{ K}$ ) and at  $1205\text{ cm}^{-1}$  (*T*<sub>2</sub> =  $873$  and  $973\text{ K}$ ), respectively (not shown).

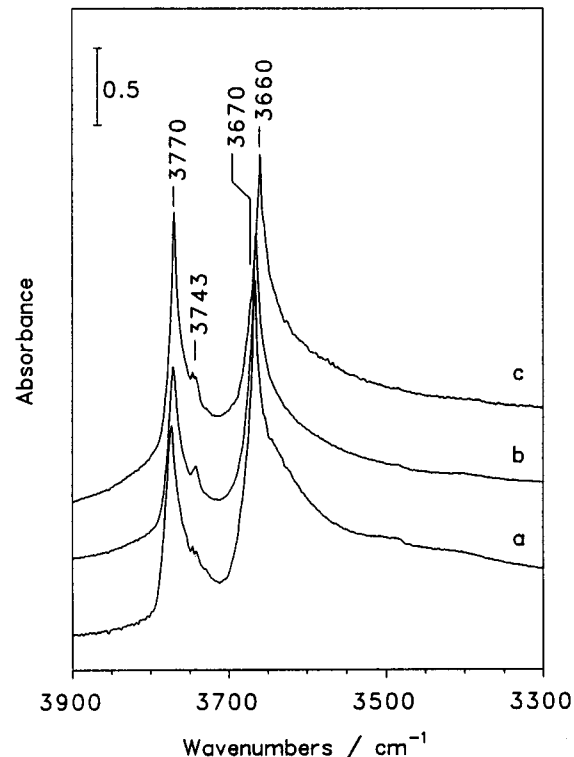


**Figure 10.** FT-IR spectra of Zr(393)P(*T*<sub>2</sub>) with (a) *T*<sub>2</sub> =  $773\text{ K}$ , (b)  $873\text{ K}$ , and (c)  $973\text{ K}$  after calcination at  $723\text{ K}$  (1 h), measured at  $77\text{ K}$ .

Addition of CO causes a shift of the band of the acidic OH–groups at  $3664\text{ cm}^{-1}$  to  $3530\text{ cm}^{-1}$  (*T*<sub>2</sub> =  $773\text{ K}$ ) and to  $3500\text{ cm}^{-1}$  (*T*<sub>2</sub> =  $873$  and  $973\text{ K}$ ), respectively (see Table 4). The increased negative shifts of the O–H stretching mode for phosphate-modified materials relative to the Zr(873) reference clearly indicate an enhanced Brønsted acid strength of the former. The increase of the protonic acidity above a calcination temperature of  $773\text{ K}$  was also found by Boyse and Ko<sup>3</sup> during calcination of ZrO<sub>2</sub>/PO<sub>4</sub> gels.

Comparing with sulfated zirconia (see Table 4), phosphate modification induces lower protonic acidity on the surface of zirconia; furthermore, basic hydroxyl groups were observed on the phosphate-modified materials in contrast to ZrO<sub>2</sub>/SO<sub>4</sub>.<sup>9</sup> It should be noted that the line widths of the Zr–OH bands of phosphate-modified zirconia are significantly decreased as compared to pure zirconia, possibly due to an enhanced separation of Zr–OH groups on ZrO<sub>2</sub>/PO<sub>4</sub> or a reduction of defects on the surface of zirconia by the modification with phosphate.

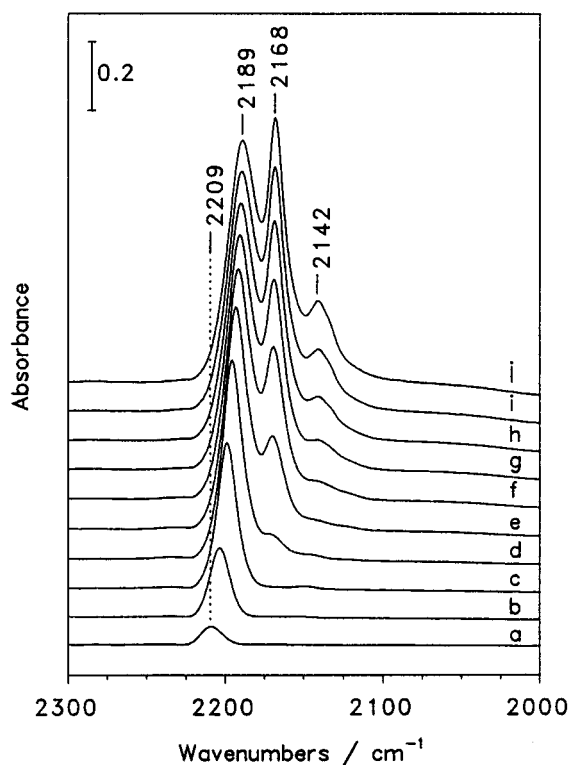
**Carbonyl Stretching Region ( $2100$ – $2250\text{ cm}^{-1}$ ).** The spectra in the CO stretching region were obtained by subtracting the (background) spectra of the CO-free samples and the gas phase spectra from the spectra of the samples with adsorbed CO. After adsorption of  $0.5\text{ mbar}$  CO on pure *m*-ZrO<sub>2</sub> Zr(873) (not shown) a band at  $2188\text{ cm}^{-1}$  was observed, which is characteristic for CO coordinated to Lewis acidic centers (Zr<sup>4+</sup>) via an interaction of the nonbonding  $5\sigma$  orbital of CO with the Zr<sup>4+</sup> center (see Table 5). At a pressure of  $1.0\text{ mbar}$  CO, the band was shifted to lower wavenumbers by an inductive effect caused by neighboring CO molecules, which is characteristic of the semiconducting oxides such as TiO<sub>2</sub>, ZrO<sub>2</sub>, and HfO<sub>2</sub>.<sup>34</sup> An additional band at  $2177\text{ cm}^{-1}$ , caused by CO adsorbed on OH groups<sup>35,36</sup> (see Table 4), is shifted to  $2168\text{ cm}^{-1}$  at higher pressures of CO. A band at  $2152\text{ cm}^{-1}$  at highest pressures of CO ( $40\text{ mbar}$ ) is indicative of physisorbed CO.

Figure 11 shows the IR spectra of the sample Zr(873)P(873).

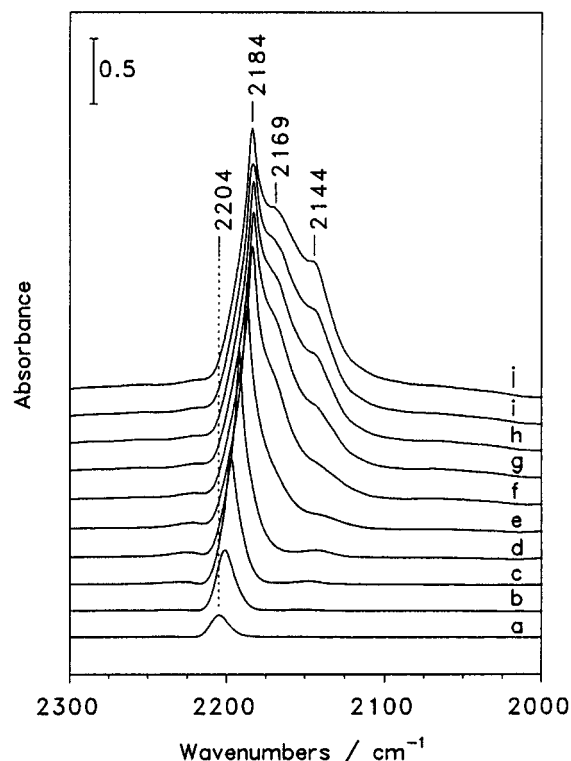
**TABLE 5: Carbonyl Stretching Frequencies of CO Adsorbed to  $\text{ZrO}_2$ ,  $\text{ZrO}_2/\text{PO}_4$ , and  $\text{ZrO}_2/\text{SO}_4$  at 77 K**

sample	$T_2/\text{K}$	$\nu_{\text{CO}}/\text{cm}^{-1}$ cus $\text{Zr}^{4+}$ <sup>a</sup>	$\nu_{\text{CO}}/\text{cm}^{-1}$ $\text{OH}^b$	$\nu_{\text{CO}}/\text{cm}^{-1}$ phys. <sup>b</sup>
Zr(873)		2188	2168	2152
Zr(873)P( $T_2$ )	773	2209	2169	2141
	873	2209	2168	2142
	973	2209	2169	2141
Zr(393)P( $T_2$ )	773	2204	2170	2146
	873	2204	2169	2144
	973	2207	2169	2144
$\text{ZrO}_2/\text{SO}_4^c$	873	2204	2166	2147
$\text{ZrO}_2/\text{SO}_4^d$	873	2204	2167	2149

<sup>a</sup> Adsorption of 55 mbar CO and subsequent evacuation at 77 K for 15 min. <sup>b</sup> Adsorption of 55 mbar CO (saturation conditions). <sup>c</sup> Prepared by calcination of sulfated  $\text{Zr}(\text{OH})_4$  at 873 K (1 h). <sup>d</sup> Prepared by calcination of sulfated Zr(873) at 873 K (1 h).

**Figure 11.** FT-IR spectra of carbonyl stretching region of Zr(873)P-(873) after calcination at 723 K (1 h) after adsorption of (a) 0.2, (b) 0.5, (c) 1.0, (d) 3.0, (e) 5.0, (f) 10, (g) 20, (h) 30, (i) 40, and (j) 55 mbar CO, measured at 77 K.

At a pressure of 0.2 mbar CO (see spectrum a in Figure 11) an asymmetric band at  $2209\text{ cm}^{-1}$  indicates the presence of CO coordinated to (different) cus  $\text{Zr}^{4+}$  centers. The shift of the carbonyl stretching vibration by about  $20\text{ cm}^{-1}$  suggests a strongly enhanced Lewis acid strength as compared to phosphate-free  $m\text{-ZrO}_2$ . Increasing the pressure of CO causes a shift of this band to  $2189\text{ cm}^{-1}$  by inductive effects<sup>34</sup> (see spectra b–j in Figure 11). Comparing these results with those obtained for sulfated zirconia<sup>9</sup> suggests that phosphate modification induces a slightly greater Lewis acid strength (see Table 5). However, inductive effects between neighboring cus  $\text{Zr}^{4+}$  centers, causing a shift of the carbonyl stretching vibration of CO coordinated to cus  $\text{Zr}^{4+}$ , are less pronounced for  $\text{ZrO}_2/\text{SO}_4$  probably due to a communication between adsorbed sulfate species and CO coordinated to cus  $\text{Zr}^{4+}$  centers.<sup>9</sup> Above 1 hPa CO, additional bands at  $2168$  and  $2142\text{ cm}^{-1}$  are obtained, which can be attributed to CO H-bonded to hydroxyl groups and physisorbed CO, respectively (see spectra d–j in Figure 11). Raising the calcination temperature  $T_2$  for samples Zr(873)P( $T_2$ ) from 773

**Figure 12.** FT-IR spectra of carbonyl stretching region of Zr(393)P-(873) after calcination at 723 K (1 h) after adsorption of (a) 0.2, (b) 0.5, (c) 1.0, (d) 3.0, (e) 5.0, (f) 10, (g) 20, (h) 30, (i) 40, and (j) 55 mbar hPa CO, measured at 77 K.

to 973 K increases the amount of Lewis acid sites (not shown), whereas their acid strength is not affected (see Table 5).

Samples Zr(393)P( $T_2$ ) show slightly reduced Lewis acid strength as compared to samples Zr(873)P( $T_2$ ) (see Table 5). Comparing the spectra of samples Zr(873)P( $T_2$ ) and Zr(393)P-( $T_2$ ) (see Figures 11 and 12, respectively, for  $T_2 = 873\text{ K}$ ) shows that the amount of Lewis acid sites, as compared to the amount of Brønsted acid sites, is higher for samples Zr(393)P( $T_2$ ). Increasing the pressure of CO causes a shift of the band for CO coordinated to cus  $\text{Zr}^{4+}$  by  $-20\text{ cm}^{-1}$  (see Figure 12), as observed for sample Zr(873)P(873).

## Concluding Remarks

Phosphate modification of  $\text{Zr}(\text{OH})_4$  retards the crystallization to  $\text{ZrO}_2$  and stabilizes the tetragonal phase of zirconia and the specific surface area of the material. Due to the high thermal stability of the adsorbed phosphate species, these effects are more pronounced as compared to sulfated  $\text{Zr}(\text{OH})_4$ . The adsorbed phosphate species, using  $\text{Zr}(\text{OH})_4$  as the precursor material, were identified by Raman, DRIFT, and  $^{31}\text{P}$ -MAS-NMR spectroscopies as pyrophosphates and doubly bridging or chelate-bonded orthophosphates. However, oligophosphates were observed after phosphate adsorption on a well-crystallized  $m\text{-ZrO}_2$ . Dehydration of  $\text{ZrO}_2/\text{PO}_4$  causes only a distortion of the geometry of the adsorbed phosphate species, whereas changes of the molecular symmetry of the sulfate species are found for  $\text{ZrO}_2/\text{SO}_4$ , due to the formation of additional  $\text{Zr}-\text{O}-\text{S}$  bonds or condensation of isolated sulfate molecules.

New hydroxyl groups, probably  $\text{P}-\text{OH}$  groups, were observed in the FT-IR spectra of  $\text{ZrO}_2/\text{PO}_4$ . Adsorption of CO shows enhanced protonic acidity as compared to pure zirconia, but lower than that of  $\text{ZrO}_2/\text{SO}_4$ . Furthermore, basic  $\text{Zr}-\text{OH}$  groups were found for  $\text{ZrO}_2/\text{PO}_4$  prepared by phosphate modification of  $\text{Zr}(\text{OH})_4$  and  $m\text{-ZrO}_2$ , whereas only acidic

hydroxyl groups were identified for the corresponding sulfated materials. While the Lewis acid strength of the observed  $\text{Zr}^{4+}$  sites is comparable to that of  $\text{ZrO}_2/\text{SO}_4$ , inductive effects between neighboring  $\text{Zr}^{4+}$  sites cause a more pronounced low-frequency shift of the carbonyl stretching vibration of CO coordinated to  $\text{Zr}^{4+}$  for phosphated zirconia, similar to the unmodified oxide. These differences are probably due to the absence of a communication between adsorbed phosphate species and the  $\text{Zr}-\text{CO}$  adsorbates, an effect that was observed on  $\text{ZrO}_2/\text{SO}_4$ .

**Acknowledgment.** This work was financially supported by the Deutsche Forschungsgemeinschaft (SFB 338), the Bayerischer Forschungsverbund Katalyse FORKAT, and the Fond der Chemischen Industrie. D.S. thanks the Studienstiftung des deutschen Volkes for a grant. G.A.H.M. acknowledges the Government of the Arab Republic of Egypt for a grant in the framework of the Channel System.

## References and Notes

- (1) Song, X.; Sayari, A. *Catal. Rev.-Sci. Eng.* **1996**, *38*, 329.
- (2) Schafer, W. A.; Carr, P. W.; Funkenbusch, E. F.; Parson, K. A. *J. Chromatogr.* **1991**, *587*, 137.
- (3) Boyse, R. A.; Ko, E. I. *Catal. Lett.* **1996**, *38*, 225.
- (4) Ciesla, U.; Schacht, S.; Stucky, G. D.; Unger, K. K.; Schüth F. *Angew. Chem., Int. Ed. Engl.* **1996**, *35*, 541.
- (5) Kraus, K. A.; Phillips, H. O. *J. Am. Chem. Soc.* **1956**, *78*, 644.
- (6) Segawa, K.; Kurusu, Y.; Nakajima, Y.; Kinoshita, M. *J. Catal.* **1985**, *94*, 491.
- (7) La Ginestra, A.; Patrono, P.; Bernadelli, M. L.; Galli, P.; Ferragina, C.; Massucci, M. A. *J. Catal.* **1987**, *103*, 346.
- (8) Clearfield, A.; Thakur, D. S. *Appl. Catal.* **1986**, *26*, 1.
- (9) Spielbauer, D.; Mekhemer, G. A. H.; Zaki, M. I.; Knözinger, H. *Catal. Lett.* **1996**, *40*, 71.
- (10) Toraya, H.; Yoshimura, M.; Somiya, S. *Commun. Am. Ceram. Soc.* **1984**, C119.
- (11) Zeilinger, H. Doctoral Thesis, Universität München, 1991.
- (12) a) Knoll, P.; Singer, R.; Kiefer, W. *Appl. Spectrosc.* **1990**, *44*, 776.  
b) Spielbauer, D. *Appl. Spectrosc.* **1995**, *49*, 650.
- (13) Beutel, T. Dissertation Universität München, 1994.
- (14) Spielbauer, D. Dissertation Universität München, 1995.
- (15) Phillipi, C. M.; Mazdiyasi, K. S. *J. Am. Ceram. Soc.* **1971**, *54*, 254.
- (16) Weidlein, J.; Müller, U.; Dehnicke, K. *Schwingungsfrequenzen I, Hauptgruppenelemente*; Georg Thieme Verlag: Stuttgart, New York, 1981.
- (17) Siebert, H. *Z. Anorg. Allg. Chemie* **1958**, *296*, 280.
- (18) Simon, A.; Richter, H. *Z. Anorg. Allg. Chemie* **1959**, *301*, 154.
- (19) Steger, E.; Leukroth, G. *Z. Anorg. Allg. Chemie* **1960**, *303*, 169.
- (20) Horsley, S. E.; Nowell, D. V.; Stewart, D. T. *Spectrochim. Acta* **1974**, *30A*, 535.
- (21) Morterra, C.; Cerrato, G.; Pinna, F.; Signoreto, M. *J. Phys. Chem.* **1994**, *98*, 12373.
- (22) Griffiths, L.; Root, A.; Harris, R. K.; Packer, K. J.; Chippendale, A. M.; Tromans, F. R. *J. Chem. Soc., Dalton Trans.* **1986**, 2247.
- (23) Duncan, T. M.; Douglass, D. C. *Chem. Phys.* **1984**, *87*, 339.
- (24) Sanz, J.; Campelo, J. M.; Marinas, J. M. *J. Catal.* **1991**, *130*, 642.
- (25) Corma, A.; Fornes, V.; Kolodziejewski, W.; Matinez-Triguero, L. *J. Catal.* **1994**, *145*, 27.
- (26) Segawa, K.; Nakajima, Y.; Nakata, S.; Asaoka, S.; Takahashi, H. *J. Catal.* **1986**, *101*, 81.
- (27) Clayden, N. J. *J. Chem. Soc., Dalton Trans.* **1987**, 1877.
- (28) Agron, P. A.; Fuller, E. L.; Holmes, H. F. *J. Colloid Interface Sci.* **1975**, *52*, 553.
- (29) Fink, P.; Pohle, W.; Köhler, A. Z. *Chem.* **1972**, *12*, 117.
- (30) Yamaguchi, T.; Nakano, Y.; Tanabe, K. *Bull. Chem. Soc. Jpn.* **1978**, *51*, 2482.
- (31) Beebe, T. P.; Gelin, P.; Yates, J. T. *Surf. Sci.* **1984**, *148*, 526.
- (32) Busca, G.; Lorenzelli, V.; Galli, P.; La Ginestra, A.; Patrono, P. *J. Chem. Soc., Faraday Trans. 1* **1987**, *83*, 853.
- (33) Marchon, B.; Novak, A. *J. Chem. Phys.* **1983**, *78*, 2105.
- (34) Bolis, V.; Morterra, C.; Fubini, B.; Ugliengo, P.; Garrone, E. *Langmuir* **1993**, *9*, 1521.
- (35) Zaki, M. I.; Knözinger, H. *J. Catal.* **1989**, *119*, 311.
- (36) Mirsojew, I.; Ernst, S.; Weitkamp, J.; Knözinger, H. *Catal. Lett.* **1994**, *24*, 235.